

## Supporting Information

**A minimal non-radiative recombination loss for efficient non-fullerene all-small-molecules organic solar cells with low energy loss of 0.54 eV and high open-circuit voltage of 1.15 V**

*Daobin Yang,<sup>a,b,†</sup> Yuming Wang,<sup>c,†</sup> Takeshi Sano,<sup>\*,a,b,d</sup> Feng Gao,<sup>\*,c</sup> Hisahiro Sasabe,<sup>\*,a,b,d</sup> and Junji Kido<sup>a,b,d</sup>*

*<sup>a</sup> Research Center for Organic Electronics (ROEL), Yamagata University, Yonezawa 992-8510, Japan*

*<sup>b</sup> Frontier Center for Organic Materials (FROM), Yamagata University, Yonezawa 992-8510, Japan*

*<sup>c</sup> Department of Physics Chemistry and Biology (IFM), Linköping University, Linköping SE-58183, Sweden*

*<sup>d</sup> Department of Organic Materials Science, Yamagata University, Yonezawa 992-8510, Japan*

*\* E-mail: takeshi.sano@yz.yamagata-u.ac.jp; feng.gao@liu.se; h-sasabe@yz.yamagata-u.ac.jp*

*† D. Yang and Y. Wang contributed equally to this work.*

### **Absorption Characterization**

Absorption spectra of the thin-film samples were recorded using a Perkin Elmer Lambda 950 UV-Vis scanning spectrophotometer. The film samples were obtained by spin-coating from chloroform solution ( $5 \text{ mg mL}^{-1}$ , 1500 rpm/40s) on quartz substrates.

**PYS Measurement:** A photoelectron yield spectroscopy (PYS) measurement system consists of a UV light source and a current measurement unit (Keithley 6430 source-measure unit). The UV light source consists of a deuterium lamp and a monochromator (JASCOSS-10) with a resolution of 3.9 nm (0.04–0.12 eV in the present wavelength region of 200–350 nm). The photon intensity distribution of this light source was measured using a calibrated photodiode (Hamamatsu Photonics S1227–1010BQ). The film samples were obtained by spin-coating from chloroform solution ( $7 \text{ mg mL}^{-1}$ , 4000 rpm/45s) on the indium-tin-oxide (ITO) glass substrates in a nitrogen-filled glove box. After spin coating, the sample was immediately moved to a vacuum chamber ( $<6 \times 10^{-3} \text{ Pa}$ ) without being exposed to air for a PYS measurement.

### **AFM Characterization**

The morphologies of the active layers were analyzed through atomic force microscopy (AFM) in tapping mode under ambient conditions using Bruker instrument. The active layers were fabricated by spin-coating (2500rpm/40s) a blend of DR3TBDTT: O-IDTBR (0.8: 1, weight ratio) in chloroform with total concentration of  $16 \text{ mg mL}^{-1}$  in a  $\text{N}_2$ -filling glovebox on the PEDOT:PSS-modified ITO substrates.

### **GI-XRD Characterization**

GI-XRD measurements were performed using a high-resolution XRD diffractometer (SmartLab, Rigaku Co.). An incident X-ray beam with a wavelength of 1.54187 Å and incident angle of 0.30° with respect to the sample plane was used. Samples were prepared on the PEDOT:PSS-treated glass substrates using identical blend solutions as those used in the devices.

### **$EQE_{EL}$ Measurement**

$EQE_{EL}$  values were obtained from an in-house-built system comprising a Hamamatsu silicon photodiode 1010B, a Keithley 2400 SourceMeter for supplying voltages and recording injected current, and a Keithley 485 picoammeter for measuring the emitted light intensity.

### **FTPS-EQE Measurement**

FTPS-EQE was measured using a Vertex 70 from Bruker Optics, equipped with a quartz tungsten halogen lamp, quartz beamsplitter and external detector option. A low-noise current amplifier (SR570) was used to amplify the photocurrent produced on illumination of the photovoltaic devices with light modulated by the Fourier transform infrared spectroscope (FTIR). The output voltage of the current amplifier was fed back into the external detector port of the FTIR, to be able to use the FTIR's software to collect the photocurrent spectrum.

### **EL measurement**

A Keithley 2400 is used for supplying the voltage/current to the devices. An Andor spectrometer (Shamrock sr-303i-B, coupled to a Newton EMCCD detector) is used to record the EL spectra.

## Mobility Characterization

Hole-only and electron-only devices are fabricated with the structure of ITO/ PEDOT:PSS (40 nm)/ DR3TBDTT: O-IDTBR (90 nm)/ MoO<sub>3</sub> (8 nm)/ Al (100 nm) and ITO/ ZnO (20 nm)/ DR3TBDTT: O-IDTBR (90 nm)/ BCP (10 nm)/ Al (100 nm), respectively. Mobility is extracted by fitting the current density-voltage curves using space charge limited current (SCLC), the  $J$ - $V$  curves of the devices are plotted as  $J^{0.5}$  versus  $V$  using the following equation:

$$J = \frac{9}{8} \frac{\varepsilon_r \times \varepsilon_0 \times \mu \times V^2}{L^3} \exp\left(0.89\beta\sqrt{\frac{V}{L}}\right)$$

where  $J$  is current density,  $L$  is film thickness of active layer,  $\mu_h$  is hole mobility,  $\mu_e$  is electron mobility,  $\varepsilon_r$  is relative dielectric constant of the transport medium,  $\varepsilon_0$  is permittivity of free space ( $8.85 \times 10^{-12}$  F m<sup>-1</sup>),  $V$  ( $= V_{\text{appl}} - V_{\text{bi}}$ ) is the internal voltage in the device, where  $V_{\text{appl}}$  is the applied voltage to the device and  $V_{\text{bi}}$  is the built-in voltage due to the relative work function difference of the two electrodes.

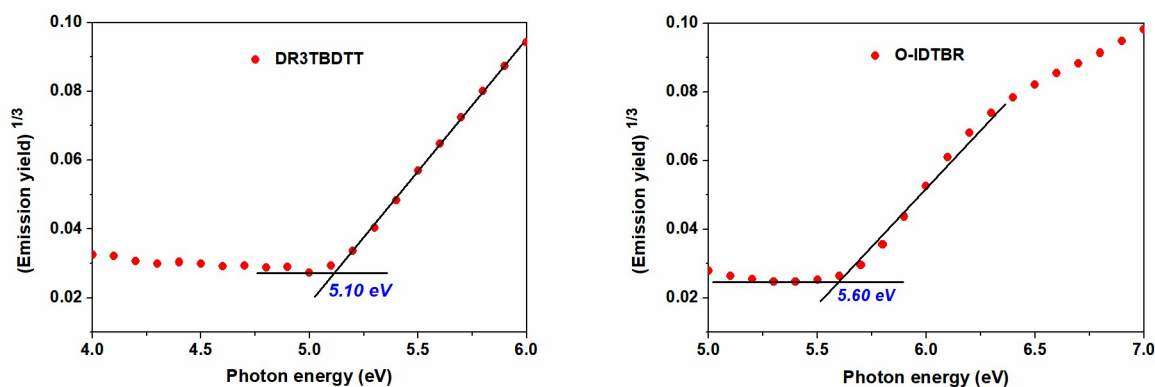


**Fig. S1.** Photoemission yield spectroscopy (PYS) spectra of DR3TBDTT and O-IDTBR films on indium-tin-oxide coated glass substrates. Emission Yield<sup>1/3</sup> is plotted against photon energy in order to estimate ionization potential (IP) of the films.

**Table S1.** Energy levels and optical band gaps for the films of DR3TBDTT and O-IDTBR.

Materials	HOMO <sup>a</sup> (eV)	LUMO <sup>b</sup> (eV)	$E_g$ <sup>c</sup> (eV)
DR3TBDTT	-5.10	-3.38	1.72
O-IDTBR	-5.60	-3.98	1.62

<sup>a</sup> HOMO values derived from PYS measurements; <sup>b</sup> LUMO =  $E_g$  + HOMO; <sup>c</sup> The optical band gaps were calculated from  $E_g = 1240 / \lambda_{\text{onset}}$ .

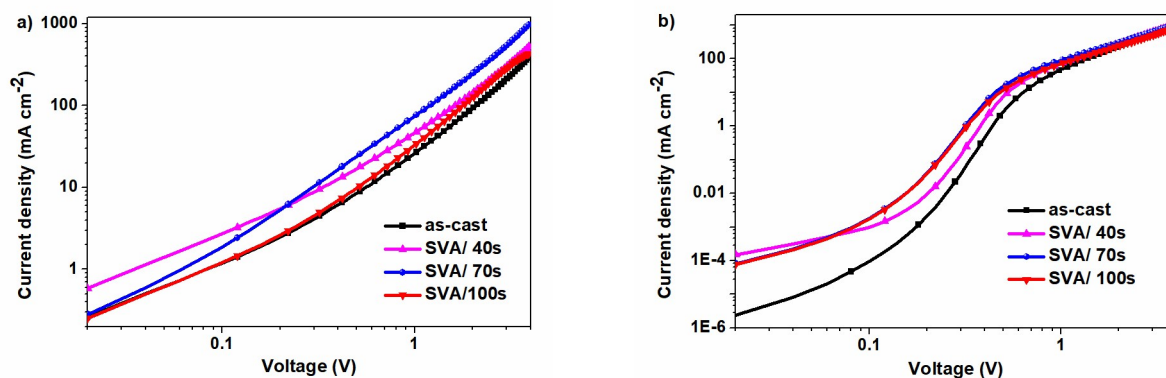


**Fig. S2.**  $J$ - $V$  characteristic of the single hole-carrier devices (a) and electron-carrier devices (b) based on DR3TBDTT: O-IDTBR (1:5, wt%) blend film with various SVA treatment.

**Table S2.** Photovoltaic performances of the NF all-SMOSCs with different blend ratios.

DR3TBDTT: O-IDTBR	$V_{oc}$ [V]	$J_{sc}$ [mA cm <sup>-2</sup> ]	FF	PCE [%]
1.25 : 1	1.14	8.47	0.425	4.12
1.00 : 1	1.16	8.52	0.433	4.29
0.80 : 1	1.16	8.67	0.430	4.34
0.67 : 1	1.17	8.68	0.417	4.22

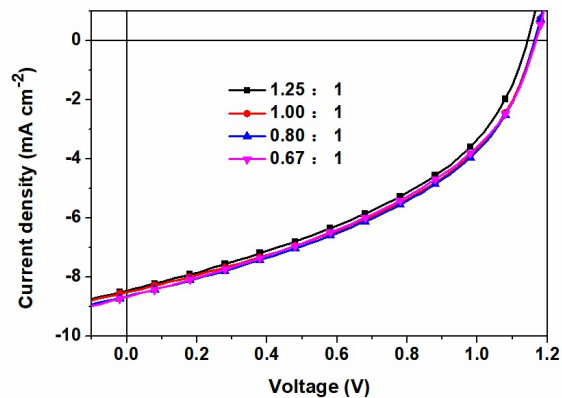


**Fig. S3.**  $J$ - $V$  curves of the NF all-SMOSCs with different blend ratios.

**Table S3.** Photovoltaic performances of the NF all-SMOSCs with different thicknesses of the active layer (D : A = 0.8 : 1).

Thickness	$V_{oc}$ [V]	$J_{sc}$ [mA cm <sup>-2</sup> ]	FF	PCE [%]
50 nm	1.16	7.41	0.438	3.77
70 nm	1.17	8.15	0.443	4.20
80 nm	1.16	8.56	0.430	4.26
90 nm	1.17	8.83	0.425	4.38

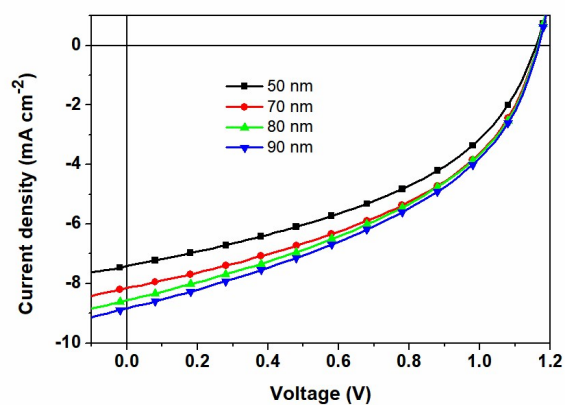


**Fig. S4.**  $J$ - $V$  curves of the NF all-SMOSCs with different thicknesses of the active layer.

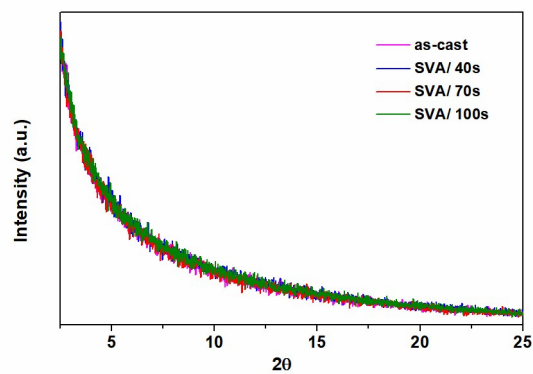


**Fig. S5.** In plane line cuts of the GI-XRD patterns for the blend films with various SVA treatment times.

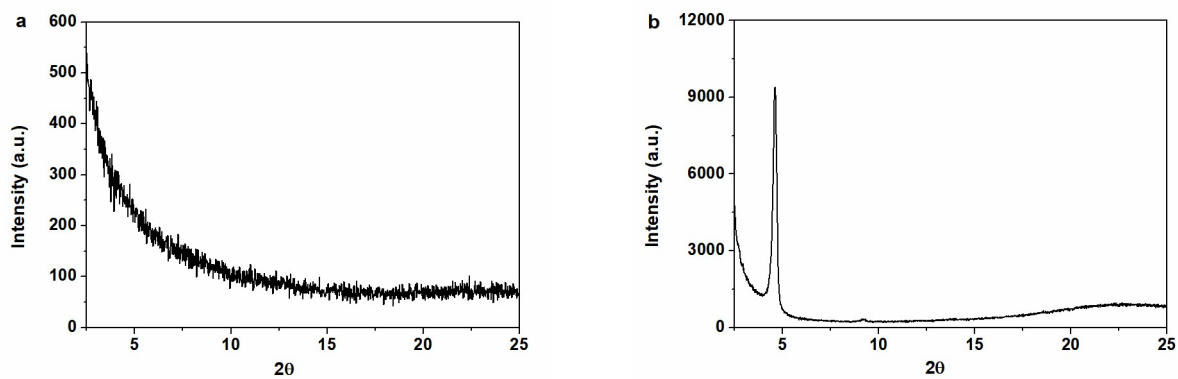


**Fig. S6.** In plane (a) and out of plane (b) line cuts of the GI-XRD patterns for the pure DR3TBDTT film.

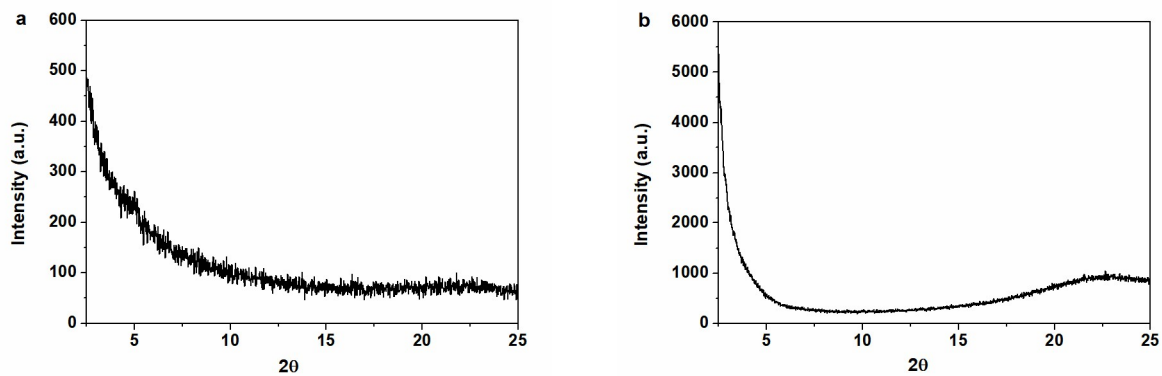


**Fig. S7.** In plane (a) and out of plane (b) line cuts of the GI-XRD patterns for the pure O-IDTBR film.

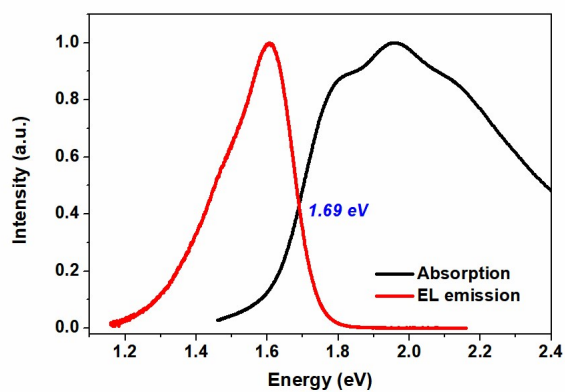


**Fig. S8.** The absorption spectra and emission spectra of blend film.

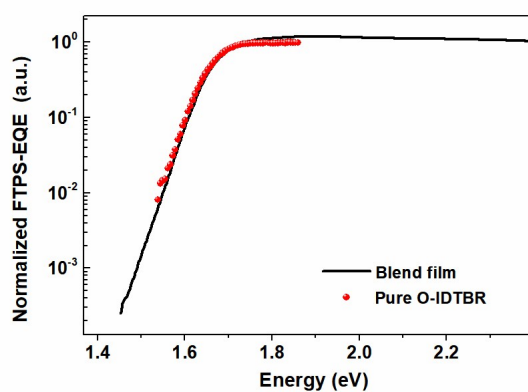


**Fig. S9.** Normalized FTPS-EQE spectra of the pure O-IDTBR and DR3TBDTT: O-IDTBR-based devices.

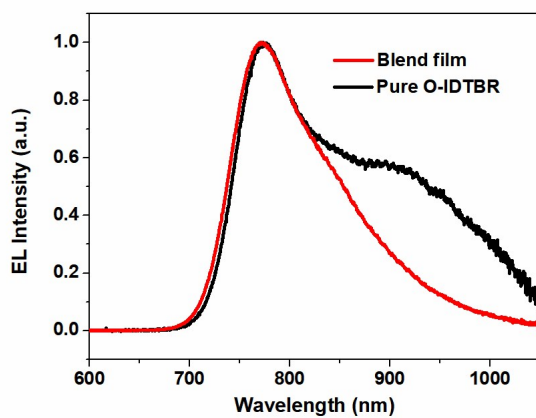


**Fig. S10.** Normalized EL spectra of the pure O-IDTBR and DR3TBDTT: O-IDTBR-based devices.



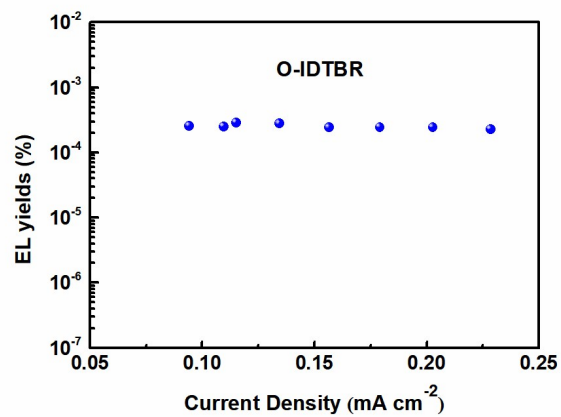
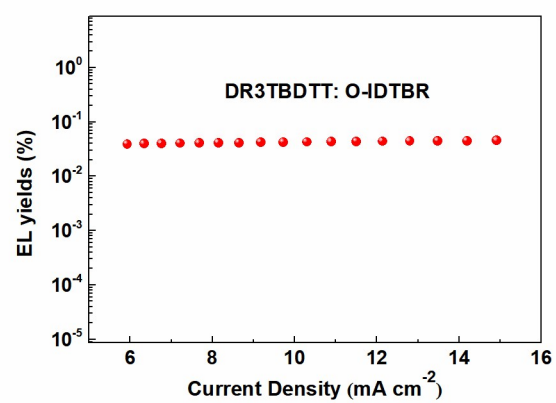


**Fig. S11.** EL yields of the pure O-IDTBR and DR3TBDTT: O-IDTBR-based devices.